A positive feedback signaling loop between ATM and the vitamin D receptor is critical for cancer chemoprevention by vitamin D

Huei-Ju Ting[1,2], Sayeda Yasmin-Karim[3], Shian-Jang Yan[2], Jong-Wei Hsu[2], Tzu-Hua Lin[2], Weisi Zeng[1], James Messing[1], Tzong-Jeng Sheu[4], Bo-Ying Bao[5], Willis Li[6], Edward Messing[1,2], and Yi-Fen Lee[1,2*]

[1]Department of Urology, [2]Pathology and Laboratory Medicine, [3]Chemical Engineering, [4]Orthopedics, University of Rochester, NY 14642; [5]School of Pharmacy, China Medical University, Taichung, Taiwan; [6]Department of Medicine, University of California, San Diego, CA 92093

*Requests for reprints should be addressed to Dr. Yi-Fen Lee, Department of Urology, University of Rochester Medical Center, 601 Elmwood Avenue, Box 656, Rochester, NY 14642; Phone: 585-275-9702, Fax: 585-756-4133, email: yifen_lee@urmc.rochester.edu

Running Title: ATM-VDR signaling in tumorigenesis

Key words: vitamin D, chemoprevention, DNA repair, phosphorylation, transcription

Abstract

Both epidemiological and laboratory studies have demonstrated the chemopreventive effects of 1-alpha,25-dihydroxyvitamin D3 (1,25-VD) in tumorigenesis. However, understanding remains incomplete concerning the molecular mechanism by which 1,25-VD prevents tumorigenesis. In this study, we used an established mouse model of chemical carcinogenesis to investigate how 1,25-VD prevents malignant transformation. In this model, 1,25-VD promoted expression of the DNA repair genes RAD50 and ATM, both of which are critical for mediating the signaling responses to DNA damage. Correspondingly, 1,25-VD protected cells from genotoxic stress and growth inhibition by promoting double strand break DNA repair. Depletion of the vitamin D receptor (VDR) reduced these genoprotective effects and drove malignant transformation that could not be prevented by 1,25-VD, defining an essential role for VDR in mediating the anti-cancer effects of 1,25-VD. Notably, genotoxic stress activated ATM and VDR through phosphorylation of VDR. Mutations in VDR at putative ATM phosphorylation sites impaired the ability of ATM to enhance VDR transactivation activity, diminishing 1,25-VD-mediated induction of ATM and RAD50 expression. Together, our findings identify a novel vitamin D-mediated chemopreventive mechanism involving a positive feedback loop between the DNA repair proteins ATM and VDR.

Introduction

The chemopreventative role of vitamin D in numerous types of cancer, including colorectal, breast, and prostate cancer was first suggested by epidemiological studies (1-3). Further studies demonstrated that vitamin D deficiency is associated with risk of cancer development (4-6). Pre-clinical studies support the chemopreventative effect of vitamin D in carcinogen-induced animal tumor models (7-9). Moreover, vitamin D receptor (VDR) deficient mice exhibit higher carcinogen-induced tumor incidence in numerous tissues (10). Therefore, vitamin D supplementation and the activation of the VDR signaling pathway protect organisms from malignant transformation.

Cells are constantly challenged by spontaneous errors as well as environmental insults that lead to DNA damage. Accumulated genomic mutations from improperly repaired DNA damages can lead to malignant transformation. Several studies indicate vitamin D attenuates DNA damage levels. Vitamin D can reduce ultraviolet light irradiation-induced DNA photoproducts, and chromosome aberrations in diethylnitrosamine-treated liver (11-13). This could result from decreasing sources of genotoxic stress, for example, the antioxidant effect of vitamin D protects cells against oxidative insults (13-16). Recently, accumulated evidence from gene profiling demonstrates that vitamin D induces the expression of DNA repair genes (17, 18) suggesting that vitamin D could facilitate DNA repair pathways.

DNA double-strand breaks (DSB), mostly caused by exposure to reactive oxygen species (ROS), ionizing radiation (IR), or generated during replication of single-strand breaks, are

susceptible to exonucleases that lead to loss of large genomic regions. Once DSB occur, formation of the Mre11/Rad50/NBS complex recruits the DDR signaling kinase, ATM (ataxia telangiectasia mutated), to the DSB, then the H2A histone family member X (H2Ax) is phosphorylated by ATM. The formation of foci containing serine 139-phosphorylated H2Ax (γ-H2Ax) is required for retaining mediator proteins, TP53BP1, MDC1, BRCA1, and the Mre11/Rad50/NBS complex at the DSB. These mediator proteins facilitate assembly of the DNA repair machinery to perform the repair of DSB (19). There are two DSB repair pathways, homologous recombination (HR) and non-homologous end joining (NHEJ). HR utilizes Holliday junction formation to facilitate strand transfer exchange between sister chromatids and is therefore less error prone. NHEJ is an efficient but more error prone repair pathway (20). Malfunctioned DNA damage response (DDR) signaling proteins and repair machineries can have catastrophic consequences that lead to premature aging and tumorigenesis (21, 22). Recent findings discovered that the DDR signaling cascades ATM-Chk2-p53 pathway is up-regulated by oncogenic stress, and inhibition of ATM leads to large and invasive tumor development (23, 24). These studies conclude that the ATM signaling pathway is an anti-cancer barrier of early stage tumorigenesis.

In the current study, we demonstrate a cross-talk between DDR and vitamin D signaling in protecting DNA from genotoxic insults which is one mechanism mediating the chemopreventative effect of vitamin D in tumorigenesis.

Materials and Methods

Plasmids and reagents. NHEJ reporter, GFP-Pem1-Ad2, was a generous gift from Dr. Vera Gorbunova (University of Rochester, Rochester, NY). pDsRed-N1 was purchased from Clontech (Mountain View, CA). Plasmids for green fluorescence protein (GFP) based HR assay system, pDR-GFP and pCβASce, were generous gifts from Dr. Maria Jasin (Memorial Sloan-Kettering Cancer Center, New York, NY). The plasmids pGEX-KG-VDR-L, pGEX-KG-VDR-L1, and pGEX-KG-VDR-L2 were constructed by PCR amplifying VDR fragments with oligomers containing BamHI and XbaI sites, which were then inserted into pGEX-KG vectors (Promega, Madison, WI). pCDNA3-flag-ATM and pCDNA-flag-ATMkd were generous gifts from Dr. Michael Kastan (St. Jude Children's Research Hospital, Memphis, TN). pCDNA-flag-VDR was constructed by PCR amplifying VDR cDNA using oligomers containing BamHI and XbaI sites, then inserted into pCDNA-flag plasmids. pCDNA-flag-mutant VDRs were constructed by QuikChange® Site-Directed Mutagenesis kit (Stratagene, La Jolla, CA). Antibodies of γ-H2Ax (clone JBW301) and phospho-ATM (serine 1981) were purchased from Millipore (Billerica, MA); H2Ax was from Bethyl Lab (Montgomery, TX); VDR (H-81), ATM, and β-actin were from Santa Cruz (Santa Cruz, CA); phosphoserine was from Zymed (San Francisco, CA). ATM specific inhibitor, KU55933, was purchased from Selkeck (Houston, TX). MEF cells from $VDR^{-/+}$ and $VDR^{-/-}$ mice were generous gifts from Dr. Jun Sun (University of Rochester Medical Center, Rochester, NY). RWPE-1 is from ATCC (Manassas, VA).

Anchorage-independent colony forming assay. BPH-1 cells were maintained in 10% FBS supplemented RPMI medium. MEFs derived from $VDR^{-/+}$ and $VDR^{-/-}$ mice were maintained in 10% FBS supplemented DMEM medium. Cells suspended at a density of 1×10^5 cells/ml in 0.4% Noble agar (Sigma, St. Louis, MO) containing medium were seeded on top of underlayer of 0.8% agarose containing medium in culture plates. Media were refreshed twice per week for three weeks. Colonies were stained with p-iodonitrotetrazolium violet (Sigma, St. Louis, MO), photographed and counted.

Xenograft mouse tumor model. The study was approved by the University of Rochester Committee on Animal Resources, and the mice were kept in a specific pathogen-free environment at the animal facility of the University of Rochester Medical Center. Young adult male athymic NCr-nu/nu mice (NCI-Frederick, Frederick, MD) at 8-10 weeks of age were subcutaneously injected with NMU transformed BPH-1 series cell lines into the dorsal lateral flank. Tumors were allowed to grow, measured weekly with calipers, and tumor volumes were calculated using the formula 0.532 x $r1^2$ x $r2$ ($r1<r2$). Mice were weighed every week. Once they reached the end point (tumor size >1 cm^3), mice from all groups were euthanized by CO_2 and cervical dislocation.

Gene profiling. After NMU-induced transformation was completed, gene expression profiles were identified by the Oligo GEArray® Human Cancer Microarray (SABioscience, Frederick, MD) according to manufacturer's manual. Briefly, RNA harvested from cells was used as template for generating biotin labeled probes. After hybridization of membranes containing cancer pathway related genes with probes, membranes were washed then developed for chemiluminescence imaging (Versadoc, BioRad). After analysis using

SABioscience online quantification software, genes with expression altered ≥1.5 fold were identified. By using GoMiner online software, altered genes between groups were functionally categorized and analyzed for statistical significance ($p<0.05$).

GFP-based NHEJ and HR assay. These assays are described in the literature for NHEJ (25) and HR reporter assay (26). In brief, for NHEJ assay, BPH-1 cells were treated with EtOH or 1,25-VD for 24 h, then transfected with GFP expression plasmids (*HindIII* digested) (0.5 μg/10^5 cells) that express GFP only after repair of digested breaks and pDsRed-N1 (0.5 μg/10^5) for transfection control. Cells were harvested two days after transfection. The efficiency of NHEJ repair was analyzed using flow cytometry to quantify GFP positive cells, which represent successful NHEJ DNA repair, and normalized by DsRed positive cells for transfection efficiency. For HR assay, BPH-1 cells were treated as described above and transfected with plasmids for HR assay (pDR-GFP and pCβASce, both at 0.5 μg/10^5). Cells transfected with pDR-GFP plasmid were selected by puromycin (2 μg/ml) for two days then harvested at 6 days after transfection. Cells were subjected to analysis of GFP positive cells under flow cytometry. Transfection was performed by the Neon™ Transfection System (Invitrogen, Carlsbad, CA). Flow cytometry was performed using FACSCanto-II (BD, Franklin Lakes, NJ) and analyzed by FlowJo software.

Establishing siRNA targeted VDR knockdown stable cell lines. Retrovirus based plasmids (pSM2c) carrying siRNA targeting VDR (siVDR) and control siRNA (SC) were purchased from Open

Biosystem (Huntsville, AL). Stable cell lines expressing these siRNAs were generated according to the manufacturer's manual (OligoEngine, Seattle, Washington).

ChIP assay. ChIP assays were performed according to a previous publication (30). DNA fragments containing VDREs in ATM and RAD50 genes were amplified by the following specific primer pairs (sequence available upon request).

In vitro kinase assay. ATM kinase assay was performed according to a previous publication (27). GST-conjugated VDR fragment proteins were isolated according to the manufacturer's manual (Promega, Madison, WI).

Immunoprecipitation and detection of phosphoserine. BPH-1 cells on 10-cm dishes were treated with KU55933 for 2 h then exposed to 1 mM H_2O_2 for 30 min, then changed to fresh normal medium. Proteins were harvested three hours after H_2O_2 challenge by RIPA buffer containing protease inhibitor (cOmplete mini, Roche, Indianapolis, IN) and phosphatase inhibitor (1 mM NaF and 1 mM NaVO3). Proteins were incubated with anti-VDR overnight at 4C, precipitated by protein A/G agarose beads (Santa Cruz), washed three times with RIPA buffer then loaded on 12% SDS-PAGE. Phosphoserine was detected by Western blotting using anti-phosphoserine and Peroxidase-IgG Fraction Monoclonal Mouse anti-rabbit IgG, light chain specific (Jackson ImmunoResearch Lab, West Grove, PA).

Cell viability assay, Quantitative PCR (Q-PCR) analysis, Western Blotting assay, Transient

transfection and luciferase assays, and DNA pull-down assay were performed according to previous publications (28, 29). Sequence of oligomers for amplifying actin, ATM and RAD50 in Q-PCR assay are available upon request.

Results

Vitamin D is chemopreventive in N-nitroso-N-methylurea (NMU) transformation model. To further investigate the chemopreventative effect of vitamin D supplement, an *in vitro* model using NMU to transform prostate epithelial cells was applied (30). BPH-1 cells, a non-malignant human prostate epithelial cell line (31), were subjected to three repeated cycles of NMU treatment, then subcultured for another six passages to select clones with significant growth advantage (Fig. 1A).

In anchorage-independent colony forming assay, BPH-1(NMU) cells formed many colonies indicating malignant transformation (Fig. 1B middle). Importantly, 1,25-VD treatment can reduce NMU-induced BPH-1 malignant transformation with fewer colonies formed (Fig .1B bottom). The tumorigenicity was further confirmed in xenografted nude mice. The result showed 60% of NMU-treated BPH-1 cells formed tumors (n=10), but none of the DMSO-treated BPH-1 cells (n=16) or 1,25-VD-pretreated NMU-BPH-1 cells (n=6) formed growing tumors (Fig. 1C). Tumor forming frequency between BPH-1(NMU) and BPH-1(VD+NMU) is 60% vs 0% ($p<0.034$, Fisher's exact test).

DNA damage signaling genes and DNA repair are promoted by 1,25-VD. In order to investigate the underlying molecular mechanism, we performed gene profiling analysis using the human Cancer Pathway SuperArray® (Supplementary Fig. 1A). We found 63 genes were altered at a magnitude ≥ 1.5 fold by vitamin D in NMU treated groups, including 23 up-regulated and 40 down-regulated

among a total of 440 genes. These genes were distributed in four statistically significant Gene Ontology (GO) categories (Supplementary Fig. 1B).

Two DSB repair genes, ATM and RAD50, were found to express higher in BPH-1(VD+NMU) compared to BPH-1(NMU) (Fig. 1B and 1C). We suspect that 1,25-VD promotes or maintains DNA DSB damage repair capacity that is altered by carcinogen and other genotoxic challenges. We examined whether 1,25-VD treatment can also promote cell recovery from NMU-induced DSB by γ-H2Ax kinetic assay. Although NMU generates DNA alkylation that is repaired mostly by base excision repair, it is also known that DSB occurs upon alkylating reagents challenge (32), and that DSB repair protects cells from genotoxicity of alkylating agents (33). We found NMU exposure increased the levels of γ-H2Ax starting from 30 min, to a maximum at 2 h in vehicle treated cells, but the NMU-induced γ-H2Ax induction was significantly reduced in the 1,25-VD treated cells (Fig. 2A). Measuring γ-H2Ax foci number found 1,25-VD can reduce NMU-induced foci numbers at 2 h after NMU exposure (Fig. 2B). This was not due to 1,25-VD altering cell cycle distribution (Supplementary Fig. 2A). We also observed the protective effect of 1,25-VD in H_2O_2 induced DSB at 6 h (Supplementary Fig. 2B). These findings that γ-H2Ax foci numbers and ATM activation (Supplementary Fig. 2C) by genotoxic insults were lower in 1,25-VD treated groups suggests 1,25-VD decreased DSB levels. RWPE-1 is another non-malignant prostate epithelial cell line in which the DNA protective effects of 1,25-VD were also observed (Supplementary Fig. 3). This could be a result of 1,25-VD reducing ROS generation as demonstrated in our previous publication (28)

and/or promoting DSB DNA repair when cells are faced with genotoxic insults.

In order to further understand whether 1,25-VD can promote DSB DNA repair, we examined the effects of 1,25-VD on two DSB repair pathways: NHEJ and HR repair. Treatment of BPH-1 cells with 1,25-VD significantly promoted the HR DNA repair capacity, as well as the NHEJ DNA repair capacity but to a lesser degree (Fig. 2C). Together, these results suggested that 1,25-VD protects cells from genotoxic insults through inducing DNA repair genes' expression to promote the repair of DSB.

VDR protect cells from genotoxicity and tumorigenesis. To explore whether VDR mediates the 1,25-VD's protective role against genotoxicity, we established siRNA VDR knocked down (BPH-1siVDR) vs scramble control (BPH-1SC) BPH-1 cell lines. VDR knockdown efficiency was 70% and VDR transactivity measured by the induction of CYP24, ATM and RAD50 expression was reduced (Fig. 3A). The protective effect of 1,25-VD against H_2O_2 and IR-induced cell death was lost in BPH-1siVDR cells compared to BPH-1SC cells (Fig. 3B, Supplementary Fig. 4A). Moreover, the effect of 1,25-VD facilitating DSB recovery could only be seen in BPH-1SC but not in BPH-1siVDR cells (Fig. 3C). All these data support VDR's role in protecting cells from genotoxicity.

Next, we examined the role of VDR in the chemopreventative effect of 1,25-VD. Knockdown of VDR sufficiently induced colony formation, representing tumorigenicity, even without NMU treatment (Fig. 3D DMSO treated BPH-1siVDR *vs* BPH-1SC). This is observed from two independent stable clones, and is therefore unlikely to result from insertion of transgenes into critical

genome sites. This result strongly supports the tumor suppressive role of VDR. However, 1,25-VD treatment can still reduce NMU-induced tumorigenecity in BPH-1siVDR cells. (The representative photos of colonies are shown in Supplementary Fig. 4B).

These results suggest that 1,25-VD has VDR independent chemopreventative effects, or can still function through the residual VDR signal amplified by ATM-VDR signaling loop during carcinogen challenges. In order to clarify whether VDR is essential mediating the chemopreventative effect of 1,25-VD, we obtained VDR null MEFs from VDR knockout mice (VDRko) to examine whether 1,25-VD can still suppress the tumorigenesis process in the absence of VDR. At the 11^{th} passages, VDRko MEFs spontaneously formed colonies in soft agar assays while VDR heterozygous deletion (VDRhet) MEFs formed very few colonies. Treatment of 1,25-VD cannot suppress VDRko MEFs from gaining colony forming ability (Fig. 3E and supplementary fig. 4C). This supports the tumor-suppressive role of VDR and suggests the tumor-suppressive effect of 1,25-VD requires the presence of VDR.

ATM phosphorylates and actives VDR transactivity. ATM kinase is a key molecule that senses DSB then activated to turn on the DDR signaling cascade. H_2O_2 exposure quickly activates ATM within 30 min at concentrations starting at 0.1 mM (Supplementary Fig. 5A). Interestingly, we observed that the 1,25-VD induced VDR transactivity was further enhanced by H_2O_2 challenge (Supplementary Fig. 5B-C).

To test if VDR is a downstream target of DDR signaling kinases upon induction of genotoxic stress stimuli, we screened for the phosphorylation motif on VDR using the web tool Scansite (scansite.mit.edu). Three putative ATM target sites were identified (Fig. 4A).

In vitro kinase assays revealed that ATM phosphorylated the VDR-L and VDR-L1 fragments both containing s208 and s222, but not the VDR-L2 (Fig. 4B, lower panel). In the sample containing ATM and VDR-L1, three phosphorylated bands were found including ATM, VDR-L1 (*), and an unknown band (#) that might be degraded VDR. ATM autophosphorylation and BRCA1 phosphorylation bands were observed as positive control.

We further mutated the putative phosphorylation sites in GST-VDR-L and GST-VDR-L1 fragment to generate GST-dmVDR-L and GST-dmVDR-L1. The result showed the phosphorylation was reduced but not completely abolished in these mutated fragments. VDR transactivation activity was enhanced by ATM but not ATM dead mutant (ATMkd) (Fig. 4C). The single serine mutated VDRs (VDRs208g and VDR s222a) and double serine mutant VDR (dmVDR) can respond to 1,25-VD-induced transactivity (Fig. 4C). However, only the dmVDR completely lost response to ATM (Fig. 4C). These results indicate ATM enhances VDR activity through phosphorylation of two amino acids, ser208 and ser222. Similarly, overexpression of ATM promotes endogenous VDR transactivity in BPH-1 cells (Fig. 4D).

We next found ATM specific inhibitor, KU55933, inhibited H_2O_2-enhanced VDR phosphorylation and transactivity (Fig. 4E-F). Therefore, DNA damage induced phosphorylation and

transactivation of VDR through ATM. We further compared the DNA binding ability of VDR and dmVDR. The result demonstrated H_2O_2 and 1,25-VD induced DNA binding ability of wild type (wt) VDR. On the other hand, dmVDR bound VDRE, but did not respond to 1,25-VD and H_2O_2 stimulation as strongly as wt VDR (Fig. 4G). Taken together, these data suggest DNA damage signals enhance VDR activity through phosphorylation at s208 and s222 by ATM.

ATM modified VDR is required for VDR cellular protective effects against H_2O_2 challenge. Based on our results demonstrating that 1,25-VD treatment can protect cells against DNA damage insult (Fig. 2) and VDR is a downstream target of the ATM cascade (Fig. 4), we then hypothesized that 1,25-VD-VDR's DNA protective effect is modulated by ATM, such that phosphorylation of VDR by ATM is critical for this protective effect.

To test this hypothesis, we compared cell survival upon H_2O_2 challenge in cells overexpressing wtVDR and dmVDR. Since the transactivity of dmVDR cannot be stimulated by ATM (Fig. 4C), dmVDR serves as a tool to delineate the cellular function of ATM phosphorylated VDR. BPH-1 cells were transiently overexpressed with VDR or dmVDR, treated with 1,25-VD for 24 h, and then exposed to H_2O_2 to determine cell survival. The results showed that cell survival was increased in BPH-1 cells overexpressing VDR, and treatment with 1,25-VD promoted cell survival.

In contrast, cells overexpressing dmVDR had a similar basal survival rate as compared to vector control cells (EtOH group) but the protective effect of 1,25-VD was lost in these dmVDR cells (Fig.

5A). The overexpression level of VDR and dmVDR mRNA and proteins were confirmed to be equivalent (Fig. 5B). In addition, we examined the expression of RAD50 induced by 1,25-VD in cells expressing various types of VDR. The expression of ATM and RAD50 was induced by 1,25-VD in BPH-1(Vector) cells and further induced in BPH-1(VDR) cells which were overexpressed with wt VDR. Interestingly, the induction of ATM and RAD50 by 1,25-VD is abolished in the BPH-1(dmVDR) cells (Fig. 5C).

To further validate ATM phosphorylated VDR is critical for 1,25-VD protective effect against genotoxicity, the different VDRs (wt vs. dmVDR) were re-expressed in BPH-1siVDR cells (Fig. 5D). The result showed 1,25-VD has no protective effect on BPH-1siVDR cells (Fig. 5D, left panel), and wt VDR re-expression rescued the protective effect of 1,25-VD (middle panel) but not dmVDR (right panel). In summary, we conclude that activation of VDR by ATM phosphorylation is essential for the DNA protective effect of 1,25-VD, and this 1,25-VD/VDR protective effect provides one functional mechanism mediating anti- tumorigenesis effect of vitamin D.

Discussion

Here we investigate the mechanisms underlying the chemopreventative effect of vitamin D in tumorigenesis. These results demonstrate that 1,25-VD treatment can protect cells from carcinogen-induced genotoxic stress via VDR mediated transcriptional up-regulation of DNA repair genes, ATM and RAD50, and thereby facilitate DSB repair. Reciprocally, DDR signaling kinase ATM phosphorylates and enhances the transactivity of VDR. Fig. 6 illustrates that activation of the ATM-VDR positive signaling loop upon carcinogen/oncogenic stress contributes to the protective effect of 1,25-VD against genomic insults-induced cell death and malignant transformation.

Currently, the effect of vitamin D supplementation in human cancer prevention is still under evaluation. One major concern for using vitamin D supplements in tumor prevention is the hypercalcemia side effect of high dosage vitamin D uptake. In this study, we found that a high concentration of 1,25-VD (100 nM) is required to prevent BPH-1 tumorigenesis. It is estimated that more than 4000 IU/kg vitamin D supplement is required to reach such dosage. However, the current physiological recommended upper limit dosage of vitamin D supplementation is 2000 IU. One possibility for this high dosage requirement in BPH-1 is that it is immortalized by SV40 T antigens which disrupts vitamin D signaling pathways by squelching p53 and/or downregulating VDR expression (34, 35). We predict the physiological concentration of 1,25-VD will be sufficient to activate the anti-tumorigenesis effect VDR in normal cells that contain functional p53 and Rb.

Therefore, the optimal dosage of vitamin D supplement required for preventing cancer needs to be further studied.

Phosphorylation of ATM putative target sites, s208 and s222, in VDR can enhance VDR transactivity that mutation of both serines in VDR (dmVDR) impairs ATM-VDR signaling loop. ATM enhances VDR transcactivity by increasing the DNA binding ability of VDR as evidenced by VDRE binding studies showing genotoxic stress induces VDR-VDRE complexes of wtVDR, but not dmVDR (Fig. 4G and Supplement Fig. 5C). As stated in the literature, casein kinase II can also phosphorylate VDR s208 (36). Phosphorylation of VDR s208 does not affect ligand binding, DNA binding, or RXR heterodimerization of VDR, but does promote the recruitment of DRIP205 as noted by the enhancement of VDR transactivity (36, 37). Therefore, we expect DRIP205 recruitment is another mechanism by which ATM enhances VDR transactivity.

The positive regulatory loop constituted by ATM-VDR led us to predict that 1,25-VD treatment will act synergistically with DDR signaling in suppressing tumorigenesis. Our study demonstrated that once the ATM-VDR loop is broken by either siVDR or dmVDR, the 1,25-VD regulation of ATM and RAD50 expression and protective effect of 1,25-VD against genotoxic challenges are lost (Fig. 3 and 5). These results support a critical role of the intact ATM-VDR loop in mediating vitamin D's DNA protective effect. Interestingly, the chemopreventative effect of 1,25-VD is not abolished by siVDR (Fig. 3). This suggests the DNA protective effect of 1,25-VD might not be the only chemopreventative mechanism of 1,25-VD. Other cancer pathways identified

in array can also contribute to the anti-tumorigenesis effect of 1,25-VD (Supplementary Fig. 1B). Remaining ATM-VDR signaling is possibly sufficient in mediating 1,25-VD regulation of other cancer pathways. Indeed, complete depletion of VDR by using VDRKO MEF abolishes the tumor-suppressive effect of 1,25-VD supports the essential role of ATM-VDR loop in mediating the anti-tumorigenesis effect of vitamin D. In addition, we challenged MEFs with NMU (3 cycles and one passage) but failed to induce more colonies (data not shown). More passages might be required to enrich the malignant population in order to examine the chemopreventative effect of vitamin D during carcinogen-induced malignant transformation. Meanwhile, we also immortalized MEFs by SV40LT. Interestingly, these immortalized MEFs from VDRko and VDRhet form colonies spontaneously. Once MEFs being transformed by SV40LT, vitamin D is no longer able to reduce their colony forming ability (data not shown). Therefore, cells should be treated with vitamin D prior malignant transformation in order to demonstrate its chemopreventive activity. On the other hand, we expect if ATM phosphorylated VDR is constitutively expressed, the chemopreventative effect of 1,25-VD could be amplified. Exploiting the ATM-VDR signaling loop by combination of 1,25-VD and ATM activator is therefore potentially a novel strategy to prevent cancer while mitigate the hypercalcemia side effects of vitamin D.

Overall, our efforts in mechanistic studies support vitamin D's role in guarding genomic integrity through regulation of genes involved in anti-oxidation (28) and DNA repair. Other potential pathways including inducing Ras signaling and suppressing anti-apoptotic genes, demand future

study. Another gene profiling study of 1,25-VD treated RWPE-1 cells identifies the WNT, Notch, NF-kB, IGF1, and inflammation signaling, those are also potential chemopreventive mechanisms of 1,25-VD worth pursuing (38). In cancer patients, the DNA protective effect of vitamin D can compromise the efficacy of therapy targeting DNA, such as radiotherapy and chemotherapy. Therefore, the status of vitamin D signaling, including the availability of ligands and receptor, could serve as a prognostic biomarker for predicting patients' response to radiotherapy and chemotherapy. On the other hand, vitamin D supplement might be one supportive treatment for protection against DNA damage caused by radiation exposure in healthy individuals. Finally, a novel vitamin D based chemopreventative strategy could be developed based on the ATM-VDR positive signaling loop.

Conflict of interest

Authors declare there is no competing financial interest in relation to the work described.

References

1. Garland C, Shekelle RB, Barrett-Connor E, Criqui MH, Rossof AH, Paul O. Dietary vitamin D and calcium and risk of colorectal cancer: a 19-year prospective study in men. Lancet. 1985;1:307-9.
2. Garland FC, Garland CF, Gorham ED, Young JF. Geographic variation in breast cancer mortality in the United States: a hypothesis involving exposure to solar radiation. Prev Med. 1990;19:614-22.
3. Schwartz GG, Hulka BS. Is vitamin D deficiency a risk factor for prostate cancer? (Hypothesis). Anticancer Res. 1990;10:1307-11.
4. Garland CF, Comstock GW, Garland FC, Helsing KJ, Shaw EK, Gorham ED. Serum 25-hydroxyvitamin D and colon cancer: eight-year prospective study. Lancet. 1989;2:1176-8.
5. Ahonen MH, Tenkanen L, Teppo L, Hakama M, Tuohimaa P. Prostate cancer risk and prediagnostic serum 25-hydroxyvitamin D levels (Finland). Cancer Causes Control. 2000;11:847-52.
6. Corder EH, Guess HA, Hulka BS, Friedman GD, Sadler M, Vollmer RT, et al. Vitamin D and prostate cancer: a prediagnostic study with stored sera. Cancer Epidemiol Biomarkers Prev. 1993;2:467-72.
7. Wood AW, Chang RL, Huang MT, Uskokovic M, Conney AH. 1 alpha, 25-Dihydroxyvitamin D3 inhibits phorbol ester-dependent chemical carcinogenesis in mouse skin. Biochem Biophys

Res Commun. 1983;116:605-11.

8. Kawaura A, Tanida N, Nishikawa M, Yamamoto I, Sawada K, Tsujiai T, et al. Inhibitory effect of 1alpha-hydroxyvitamin D3 on N-methyl-N'-nitro-N-nitrosoguanidine-induced gastrointestinal carcinogenesis in Wistar rats. Cancer Lett. 1998;122:227-30.

9. Lucia MS, Anzano MA, Slayter MV, Anver MR, Green DM, Shrader MW, et al. Chemopreventive activity of tamoxifen, N-(4-hydroxyphenyl)retinamide, and the vitamin D analogue Ro24-5531 for androgen-promoted carcinomas of the rat seminal vesicle and prostate. Cancer Res. 1995;55:5621-7.

10. Zinser GM, Suckow M, Welsh J. Vitamin D receptor (VDR) ablation alters carcinogen-induced tumorigenesis in mammary gland, epidermis and lymphoid tissues. J Steroid Biochem Mol Biol. 2005;97:153-64.

11. De Haes P, Garmyn M, Verstuyf A, De Clercq P, Vandewalle M, Degreef H, et al. 1,25-Dihydroxyvitamin D3 and analogues protect primary human keratinocytes against UVB-induced DNA damage. J Photochem Photobiol B. 2005;78:141-8.

12. Wong G, Gupta R, Dixon KM, Deo SS, Choong SM, Halliday GM, et al. 1,25-Dihydroxyvitamin D and three low-calcemic analogs decrease UV-induced DNA damage via the rapid response pathway. J Steroid Biochem Mol Biol. 2004;89-90:567-70.

13. Chatterjee M. Vitamin D and genomic stability. Mutat Res. 2001;475:69-87.

14. Hanada K, Sawamura D, Nakano H, Hashimoto I. Possible role of 1,25-dihydroxyvitamin

D3-induced metallothionein in photoprotection against UVB injury in mouse skin and cultured rat keratinocytes. J Dermatol Sci. 1995;9:203-8.

15. De Haes P, Garmyn M, Degreef H, Vantieghem K, Bouillon R, Segaert S. 1,25-Dihydroxyvitamin D3 inhibits ultraviolet B-induced apoptosis, Jun kinase activation, and interleukin-6 production in primary human keratinocytes. J Cell Biochem. 2003;89:663-73.

16. Banakar MC, Paramasivan SK, Chattopadhyay MB, Datta S, Chakraborty P, Chatterjee M, et al. 1alpha, 25-dihydroxyvitamin D3 prevents DNA damage and restores antioxidant enzymes in rat hepatocarcinogenesis induced by diethylnitrosamine and promoted by phenobarbital. World J Gastroenterol. 2004;10:1268-75.

17. Krishnan AV, Shinghal R, Raghavachari N, Brooks JD, Peehl DM, Feldman D. Analysis of vitamin D-regulated gene expression in LNCaP human prostate cancer cells using cDNA microarrays. Prostate. 2004;59:243-51.

18. Wu-Wong JR, Nakane M, Ma J, Ruan X, Kroeger PE. Effects of Vitamin D analogs on gene expression profiling in human coronary artery smooth muscle cells. Atherosclerosis. 2006;186:20-8.

19. O'Driscoll M, Jeggo PA. CsA can induce DNA double-strand breaks: implications for BMT regimens particularly for individuals with defective DNA repair. Bone Marrow Transplant. 2008;41:983-9.

20. Takata M, Sasaki MS, Sonoda E, Morrison C, Hashimoto M, Utsumi H, et al. Homologous

recombination and non-homologous end-joining pathways of DNA double-strand break repair have overlapping roles in the maintenance of chromosomal integrity in vertebrate cells. Embo J. 1998;17:5497-508.

21. Hoeijmakers JH. Genome maintenance mechanisms for preventing cancer. Nature. 2001;411:366-74.

22. Park Y, Gerson SL. DNA repair defects in stem cell function and aging. Annu Rev Med. 2005;56:495-508.

23. Bartkova J, Horejsi Z, Koed K, Kramer A, Tort F, Zieger K, et al. DNA damage response as a candidate anti-cancer barrier in early human tumorigenesis. Nature. 2005;434:864-70.

24. Bartkova J, Rezaei N, Liontos M, Karakaidos P, Kletsas D, Issaeva N, et al. Oncogene-induced senescence is part of the tumorigenesis barrier imposed by DNA damage checkpoints. Nature. 2006;444:633-7.

25. Seluanov A, Mittelman D, Pereira-Smith OM, Wilson JH, Gorbunova V. DNA end joining becomes less efficient and more error-prone during cellular senescence. Proc Natl Acad Sci U S A. 2004;101:7624-9.

26. Pierce AJ, Johnson RD, Thompson LH, Jasin M. XRCC3 promotes homology-directed repair of DNA damage in mammalian cells. Genes Dev. 1999;13:2633-8.

27. Kim ST, Lim DS, Canman CE, Kastan MB. Substrate specificities and identification of putative substrates of ATM kinase family members. J Biol Chem. 1999;274:37538-43.

28. Bao BY, Ting HJ, Hsu JW, Lee YF. Protective role of 1 alpha, 25-dihydroxyvitamin D3 against oxidative stress in nonmalignant human prostate epithelial cells. Int J Cancer. 2008;122:2699-706.

29. Ting HJ, Bao BY, Reeder JE, Messing EM, Lee YF. Increased expression of corepressors in aggressive androgen-independent prostate cancer cells results in loss of 1alpha,25-dihydroxyvitamin D3 responsiveness. Mol Cancer Res. 2007;5:967-80.

30. Rhim JS, Jin S, Jung M, Thraves PJ, Kuettel MR, Webber MM, et al. Malignant transformation of human prostate epithelial cells by N-nitroso-N-methylurea. Cancer Res. 1997;57:576-80.

31. Hayward SW, Dahiya R, Cunha GR, Bartek J, Deshpande N, Narayan P. Establishment and characterization of an immortalized but non-transformed human prostate epithelial cell line: BPH-1. In Vitro Cell Dev Biol Anim. 1995;31:14-24.

32. Staszewski O, Nikolova T, Kaina B. Kinetics of gamma-H2AX focus formation upon treatment of cells with UV light and alkylating agents. Environ Mol Mutagen. 2008;49:734-40.

33. Tsaryk R, Fabian K, Thacker J, Kaina B. Xrcc2 deficiency sensitizes cells to apoptosis by MNNG and the alkylating anticancer drugs temozolomide, fotemustine and mafosfamide. Cancer Lett. 2006;239:305-13.

34. Maruyama R, Aoki F, Toyota M, Sasaki Y, Akashi H, Mita H, et al. Comparative genome analysis identifies the vitamin D receptor gene as a direct target of p53-mediated transcriptional activation. Cancer Res. 2006;66:4574-83.

35. Kemmis CM, Welsh J. Mammary epithelial cell transformation is associated with deregulation of the vitamin D pathway. J Cell Biochem. 2008;105:980-8.

36. Jurutka PW, Hsieh JC, Nakajima S, Haussler CA, Whitfield GK, Haussler MR. Human vitamin D receptor phosphorylation by casein kinase II at Ser-208 potentiates transcriptional activation. Proc Natl Acad Sci U S A. 1996;93:3519-24.

37. Arriagada G, Paredes R, Olate J, van Wijnen A, Lian JB, Stein GS, et al. Phosphorylation at serine 208 of the 1alpha,25-dihydroxy Vitamin D3 receptor modulates the interaction with transcriptional coactivators. J Steroid Biochem Mol Biol. 2007;103:425-9.

38. Kovalenko PL, Zhang Z, Cui M, Clinton SK, Fleet JC. 1,25 dihydroxyvitamin D-mediated orchestration of anticancer, transcript-level effects in the immortalized, non-transformed prostate epithelial cell line, RWPE1. BMC Genomics.11:26.

Titles and legends to figures

Fig. 1. Pre-treatment with 1,25-VD prevented cell transformation. BPH-1 cells were seeded at 3×10^4 cells/dish in 60-mm dishes. (A) Diagram of NMU-induced transformation procedure. Cells were treated with ethanol (EtOH) or 100 nM 1,25-VD for 24 h then exposed to 100 μg/ml NMU for 1 h. The same treatment was repeated for another 2 times. After 6 times subculture, soft agar colony forming assays were performed. (B) Representative colony formation of cells with indicated treatment from triplicate experiments were shown. (C) BPH-1 sublines at 10^6 cells/100μl matrigel were subcutaneously injected into nude mice. Tumor volumes of BPH-1(DMSO), BPH-1(NMU), and BPH-1(VD+NMU) groups were measured as described in Methods and mean ± S.D. of three xenograft tumors plotted. * $p<0.05$ BPH-1(VD+NMU) cell xenograft tumors compared to BPH-1(NMU) cell xenograft tumors.

Fig. 2. 1,25-VD protects cells from DSB and promotes DSB DNA repair. (A) 1,25-VD promotes cells recovery from NMU-induced DSB. BPH-1 cells were incubated with vehicle or 100 nM 1,25-VD for 24 h, and then exposed to NMU (100 μg/μl) for 1 h. DNA DSB marker γ-H2Ax was detected at designated time points by Western blotting. After being normalized with H2Ax, the relative intensity of γ-H2Ax to 0 h was calculated and plotted. * $p<0.05$; ** $p<0.01$ compared to EtOH treated group at the same time point. (B) BPH-1 cells were seeded at 10^4 cells/well on chamber slide then treated with EtOH or 100 nM 1,25-VD the next day. After 24 h, cells were treated with or without H_2O_2 (0.1 mM) for 30 min then replenished with fresh medium containing EtOH or

1,25-VD. Cells were fixed at indicated time points and processed for staining with antibody of γ-H2Ax. Pictures were taken under confocal microscopy and representative pictures were shown (scale bar = 15 μm). Foci number were counted, then average foci number/cell ± S.D. were plotted. ** $p<0.01$. (C) 1,25-VD promotes NHEJ and HR repair. BPH-1 cells were treated with EtOH or 100 nM 1,25-VD for 24 h then cotransfected with *Hind*III-digested NHEJ reporter and DsRed expressing vector (NHEJ assay) or pDR-GFP and pCβASce plasmids (HR assay). Cells were continuously treated with EtOH or 1,25-VD until harvest. The percentage of GFP+ and DsRed+ cells were determined by FACS analysis. The relative repair efficiency was calculated by comparing to EtOH treated group. *: $p<0.05$; **: $p<0.01$, compared to EtOH group (n=3).

Fig. 3. The protective effect of 1,25-VD against genotoxic challenges in VDR depleted cells. (A) 1,25-VD induced gene expression in VDR depleted cells. BPH-1SC and BPH-1siVDR cells were treated with EtOH or 100 nM 1,25-VD for 24 h, then harvested for RNA extraction. The expression of indicated genes was measured by Q-PCR. The relative expression compared to BPH-1SC treated with EtOH was calculated and mean ± S.D. plotted. (B) The protective effect of 1,25-VD against genotoxicity in VDR depleted cells. BPH-1SC and BPH-1siVDR cells were treated with 100 nM 1,25-VD for 24 h, then exposed to different doses of H_2O_2. After 6 days, MTT assays were performed. Percentages of surviving cells in each treatment group compared to no H_2O_2 exposure were calculated (* $p<0.05$ compared to EtOH with same dosage of H_2O_2 treated group; n=3). (C) The effects of 1,25-VD on genotoxic agents-induced DSBs. BPH-1SC2 or BPH-1siVDR cells were

incubated with EtOH or 100 nM 1,25-VD for 24 h, and then exposed to H_2O_2 (0.1 mM) for 30′. At designated time points proteins were harvested for detecting γ-H2Ax level. The relative intensity of γ-H2Ax (normalized by actin) compared to 0 h was calculated and plotted. * $p<0.05$ compared to EtOH treated groups at the same time points. (D) The chemopreventative effect of 1,25-VD in VDR depleted cells. NMU-induced malignant transformation was performed in BPH-1sc and BPH-1siVDR cells as in Fig. 1A. Soft agar colony formation assay was performed for examining tumorigenecity. Colony numbers were counted and averaged from 9 different fields of each well under microscope at 50X magnification. Average colony numbers from two independent experiments of two independent clones of BPH-1SC and BPH-1siVDR stable cell lines were calculated and mean ± S.D. plotted. (E) MEF cells from VDRhet and VDRko mice were analyzed for their tumorigenecity after EtOH or 100 nM 1,25-VD treatment for 24 h for 3 times. Colony numbers were counted and accumulated from 10 different fields of each well under microscope. Average colony numbers from three independent counting were calculated and mean ± S.D. plotted.

Fig. 4. ATM enhanced VDR transactivity through phosphorylation. (A) Illustration of three potential ATM phosphorylation sites on VDR (AF-2, activation function domain 2). (B) ATM phosphorylated VDR fragment containing s208 and s222. GST-VDR fragments (designed as in diagram, s=serine, g=glycine, a=alanine) and GST-BRCA1 fragments were expressed and purified from bacteria (upper panel). Flag-ATM and flag-ATMkd were expressed in 293T cells,

immunoprecipitated by M2-agarose beads, then incubated with purified GST proteins in the presence of [γ-^{32}P]ATP. After reaction, samples were separated by electrophoresis, and phosphorylated proteins were detected by phosphorimager (lower panel). Three independent experiments were performed, the representative result is shown. (*= GST-VDR-L, #= possibly degraded GST-VDR-L), (C) CV-1 cells were co-transfected with wt VDR or mutant VDRs, ATM or ATMkd expression plasmids together with prCYP24-LUC. After overnight transfection, EtOH or 10 nM 1,25-VD was added for another 24 h. Cells were harvested for LUC assay. The relative LUC activity compared to VDR+flag+EtOH group was calculated and mean ± S.D. plotted. *, $p< 0.05$ ($n>3$). (D) BPH-1 cells were co-transfected with ATM or ATMkd expression plasmids (0.6 μg) together with prCYP24-LUC (0.2 μg) per well of 24-well plate. After overnight transfection, EtOH or 100 nM 1,25-VD was added for another 24 h. Cells were harvested for LUC assay. The relative LUC activity compared to EtOH group was calculated and mean ± S.D. plotted. *, $p< 0.05$ ($n=3$). (E) BPH-1 cells were treated with DMSO or KU55933 (10 μM) for 2 h then exposed to H_2O_2 (1 mM). VDR was immunoprecipitated by antibody then p-Ser and VDR were detected by Western blotting. (F) BPH-1 cells were transfected with pCYP24-LUC and pRL-SV40, and allowed to recover for 16 h. Cells were then treated with DMSO or KU55933 for 2 h then exposed to 0.1 mM H_2O_2 for 30 min, washed and allowed to recover for indicated times, then treated with 1,25-VD for 24 h for LUC assay. The relative LUC activity compared to EtOH group was calculated and mean ± S.D. plotted ($n>3$). *: $p<0.05$. (G) BPH-1siVDR cells were transfected with VDR, wt or mutant, by electroporation. Cells

were treated with or without 1 mM H_2O_2 for 30 min, and changed to fresh medium. After 2 h, cells were treated with 1,25-VD (100 nM) for 2 h before harvesting proteins. VDR-VDRE complex were pulled-down and VDR was detected by Western blotting. VDR input amount were detected in 30% input proteins of each sample.

Fig. 5. The protective effect of 1,25-VD was lost in cells expressing dmVDR. (A) BPH-1 cells were transfected with vector, VDR, or dmVDR expressing vectors. After 1,25-VD treatment for 24 h, cells were exposed to different concentrations of H_2O_2. Surviving cells were measured by MTT assay. The survival cell percentages relative to no H_2O_2 treatment were calculated and mean ± S.D. plotted. * $p<0.5$, ** $p<0.01$ (n=3). (B) BPH-1 cells were infected with retrovirus carrying control vector, dmVDR, or VDR expressing vector. The expression of VDR was measured by Q-PCR (upper panel) and Western blotting (lower panel). (C) Transfected cells were treated with EtOH or 100 nM 1,25-VD for 24 h. The expression of ATM and RAD50 mRNA was measured by Q-PCR. The relative expression compared to BPH-1(vector) treated with EtOH was calculated and mean ± S.D. plotted. *$p<0.05$ (n=3). The mRNA expression level of VDR was measured by Q-PCR assays. The relative expression level of VDR compared to BPH-1(vector) was calculated and mean ± S.D. plotted. (D) As described in (A), the protective effect of 1,25-VD in wt or dmVDR overexpressed BPH-1siVDR cells were examined. * $p<0.5$, (n=3).

Fig. 6. Schematic diagram of DNA protective and anti-tumorigenesis mechanism of ATM-VDR signaling axis. Carcinogen and other oncogenic stress can stimulate ATM triggering DDR signaling

cascade to activate p53 and other factors in forming anti-cancer barrier in early stage cancer initiation. Activated ATM can also phosphorylate and enhance VDR transactivity in regulating expression of ATM and RAD50 hence promotes DSB repair guarding genome integrity. Other anti-cancer pathway, such as senescence and apoptosis, are potentially regulated by 1,25-VD-VDR signaling.

Fig. 1

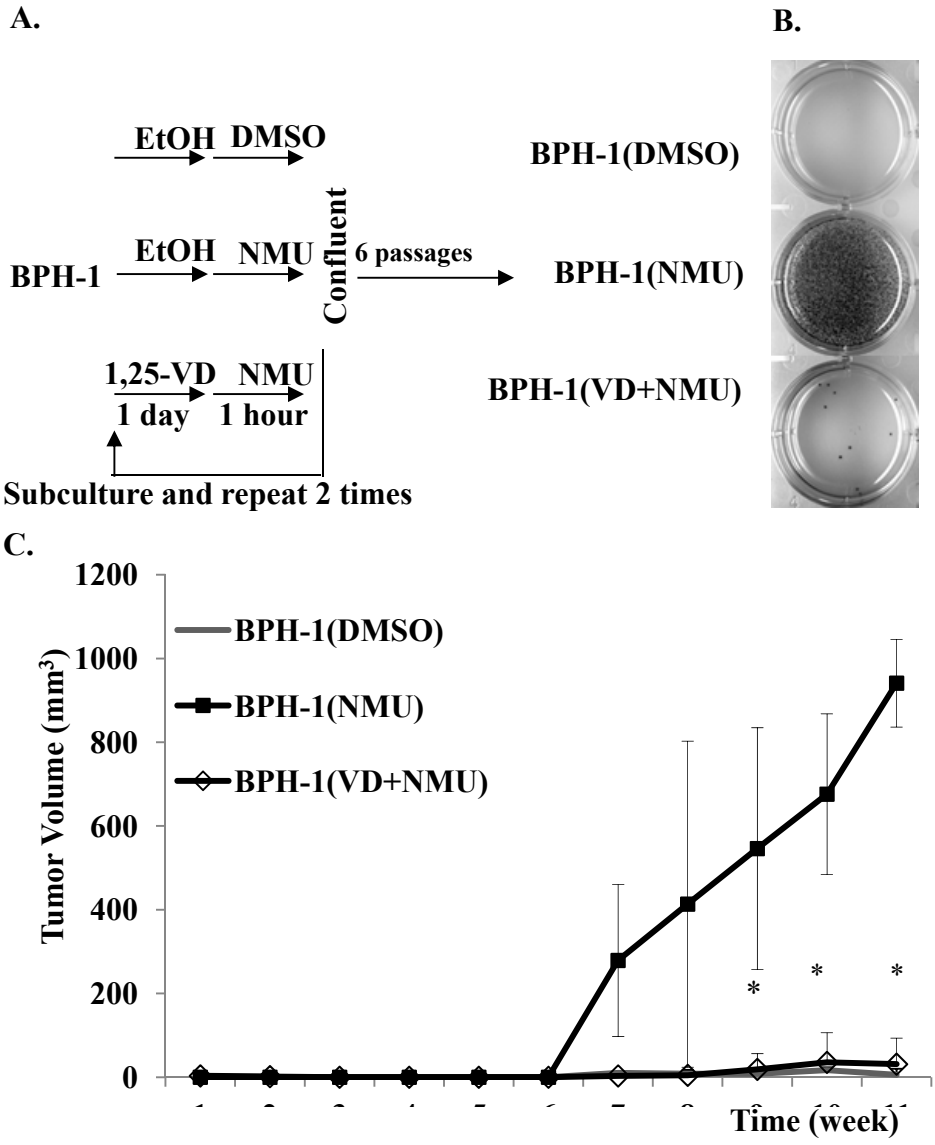
A.
B.
EtOH
DMSO
BPH-1(DMSO)
BPH-1
EtOH
NMU
Confluent
6 passages
BPH-1(NMU)
1,25-VD
NMU
1 day
1 hour
BPH-1(VD+NMU)
Subculture and repeat 2 times
C.
1200
1000
800
600
400
200
0
Tumor Volume (mm3)
BPH-1(DMSO)
BPH-1(NMU)
BPH-1(VD+NMU)
*
*
*
Time (week)

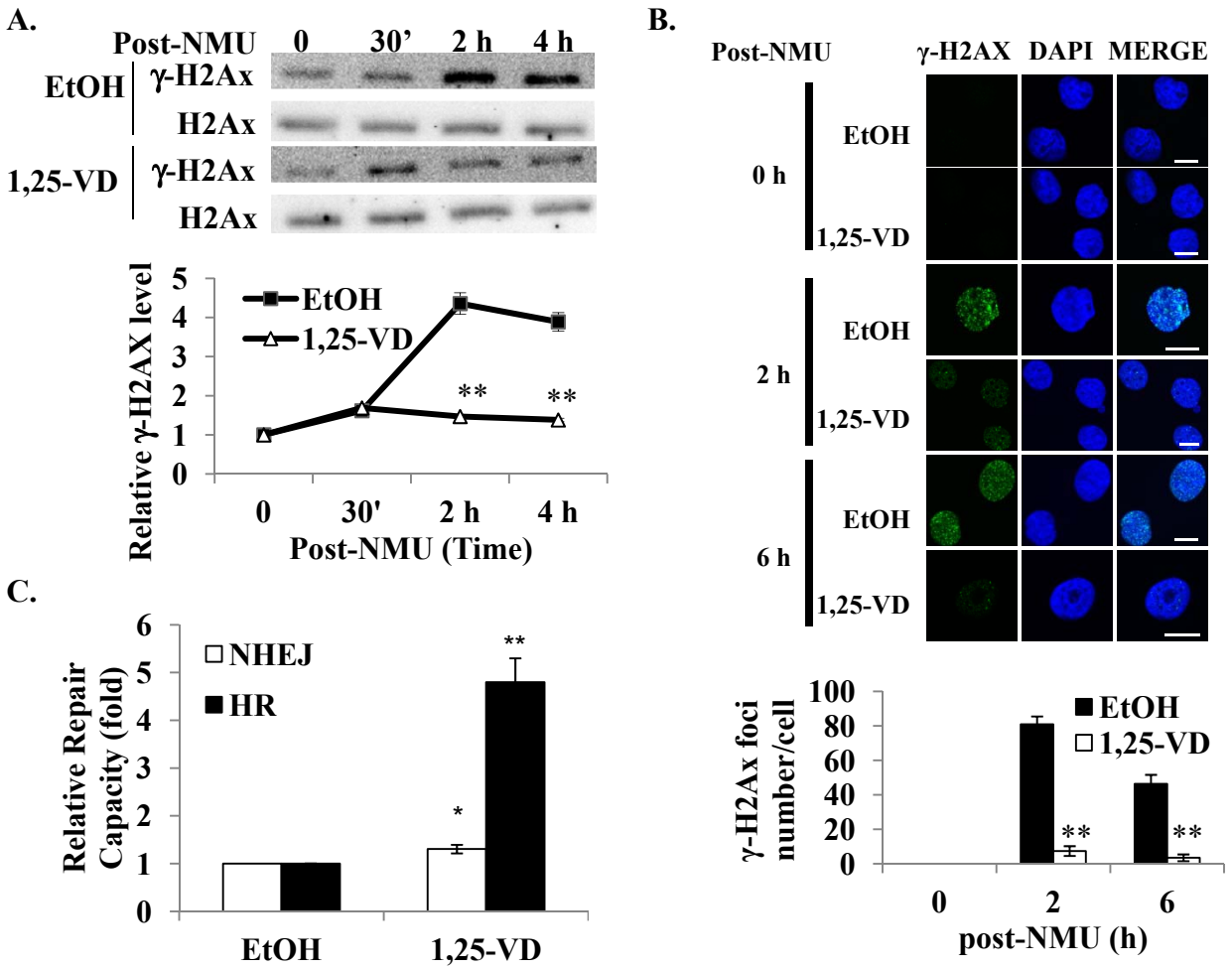
A.
Post-NMU
0
30'
2 h
4 h
EtOH
γ-H2Ax
H2Ax
1,25-VD
γ-H2Ax
H2Ax
Relative γ-H2AX level
EtOH
1,25-VD
**
**
Post-NMU (Time)
B.
Post-NMU
γ-H2AX
DAPI
MERGE
0 h
2 h
6 h
EtOH
1,25-VD
γ-H2Ax foci number/cell
post-NMU (h)
C.
Relative Repair Capacity (fold)
NHEJ
HR
*
**
EtOH
1,25-VD

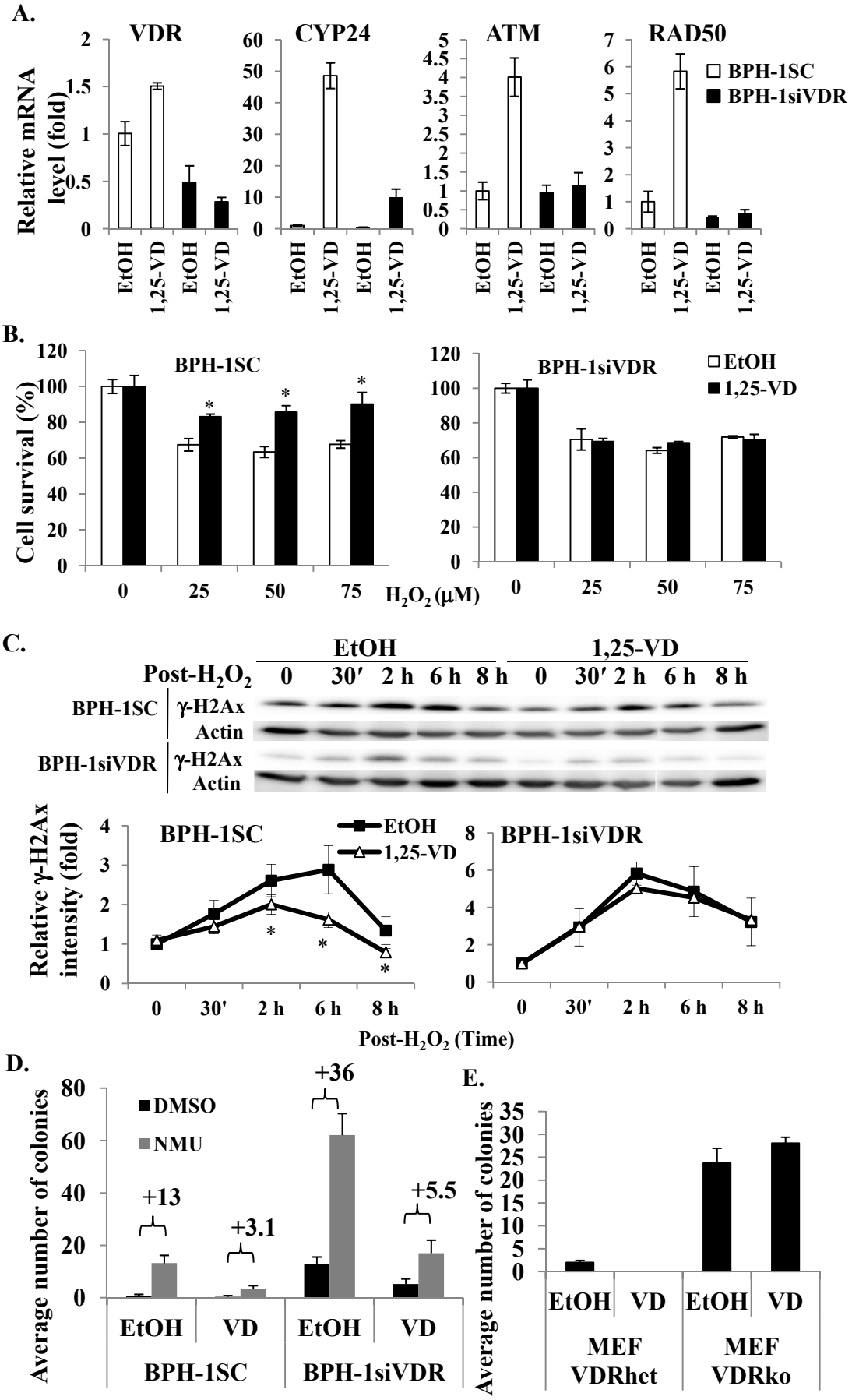
A.
VDR
CYP24
ATM
RAD50
Relative mRNA level (fold)
BPH-1SC
BPH-1siVDR
EtOH
1,25-VD
B.
BPH-1SC
BPH-1siVDR
Cell survival (%)
H2O2 (μM)
C.
EtOH
1,25-VD
Post-H2O2
0
30′
2 h
6 h
8 h
BPH-1SC
γ-H2Ax
Actin
BPH-1siVDR
Relative γ-H2Ax intensity (fold)
Post-H2O2 (Time)
D.
DMSO
NMU
+13
+3.1
+36
+5.5
Average number of colonies
BPH-1SC
BPH-1siVDR
E.
MEF VDRhet
MEF VDRko

Fig. 4

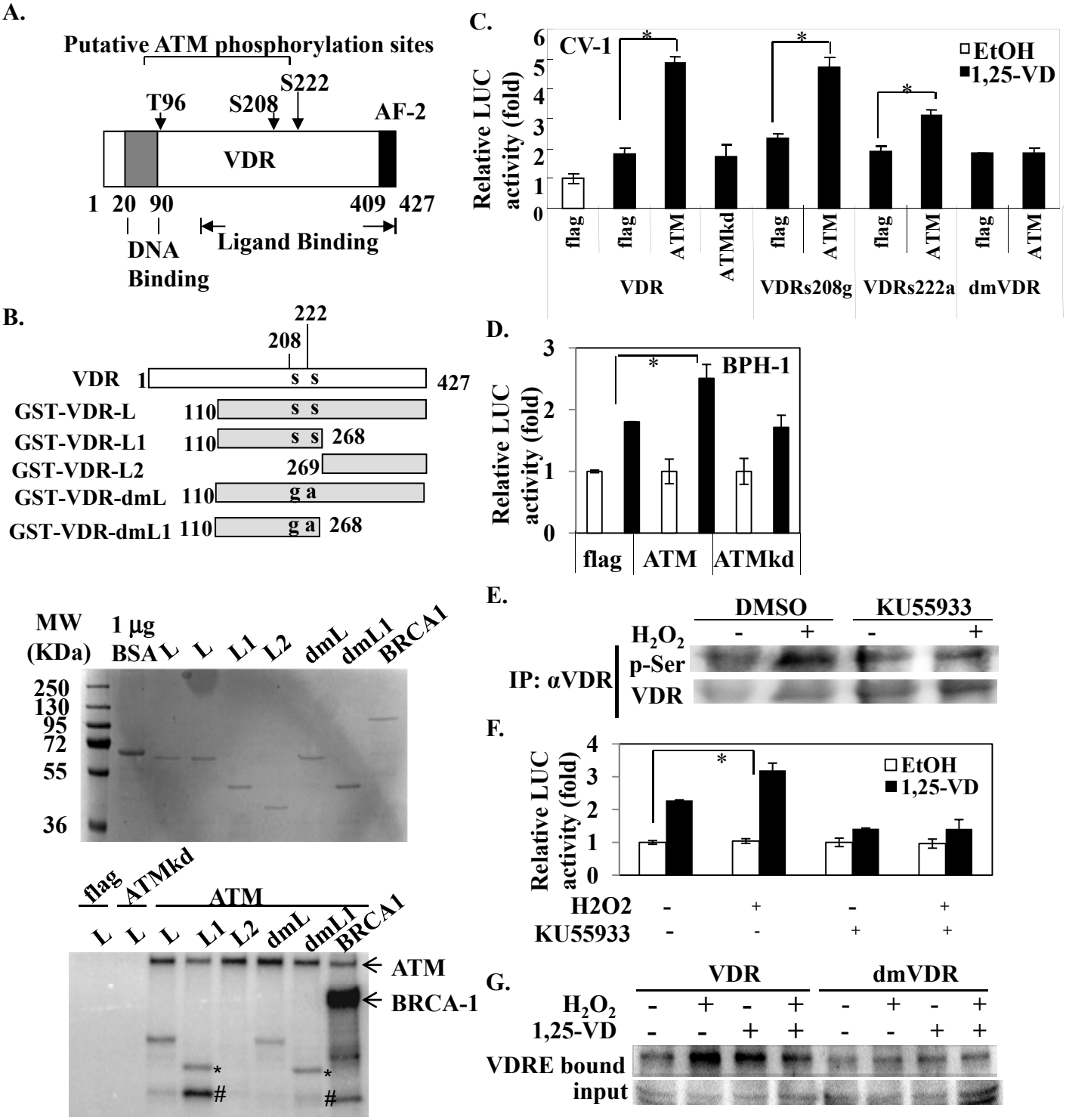
A.
Putative ATM phosphorylation sites
T96
S208
S222
AF-2
VDR
1 20 90 409 427
DNA Binding
Ligand Binding
B.
222
208
VDR 1 s s 427
GST-VDR-L 110 s s
GST-VDR-L1 110 s s 268
GST-VDR-L2 269
GST-VDR-dmL 110 g a
GST-VDR-dmL1 110 g a 268
C.
CV-1
EtOH
1,25-VD
Relative LUC activity (fold)
flag
ATM
ATMkd
VDR
VDRs208g
VDRs222a
dmVDR
D.
BPH-1
Relative LUC activity (fold)
flag
ATM
ATMkd
MW (KDa)
1 µg BSA
L
L1
L2
dmL
dmL1
BRCA1
250
130
95
72
55
36
ATM
BRCA-1
E.
DMSO
KU55933
H2O2
IP: αVDR
p-Ser
VDR
F.
EtOH
1,25-VD
Relative LUC activity (fold)
H2O2
KU55933
G.
VDR
dmVDR
H2O2
1,25-VD
VDRE bound
input

Fig. 5

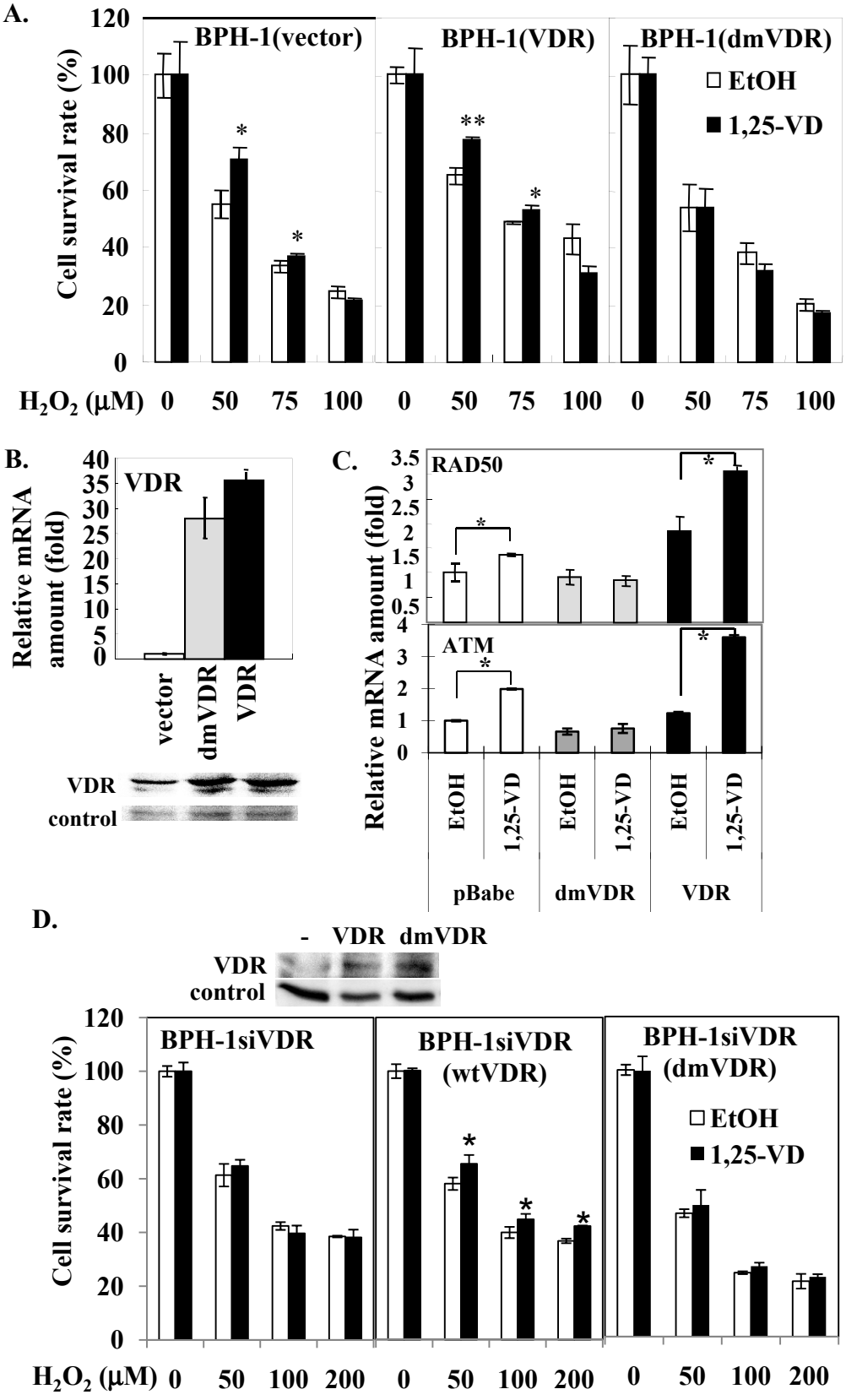
A.
BPH-1(vector)
BPH-1(VDR)
BPH-1(dmVDR)
EtOH
1,25-VD
Cell survival rate (%)
H2O2 (μM) 0 50 75 100 0 50 75 100 0 50 75 100
B.
Relative mRNA amount (fold)
VDR
vector
dmVDR
VDR
VDR
control
C.
RAD50
ATM
Relative mRNA amount (fold)
EtOH
1,25-VD
pBabe
dmVDR
VDR
D.
- VDR dmVDR
VDR
control
BPH-1siVDR
BPH-1siVDR (wtVDR)
BPH-1siVDR (dmVDR)
Cell survival rate (%)
H2O2 (μM) 0 50 100 200 0 50 100 200 0 50 100 200

Fig. 6

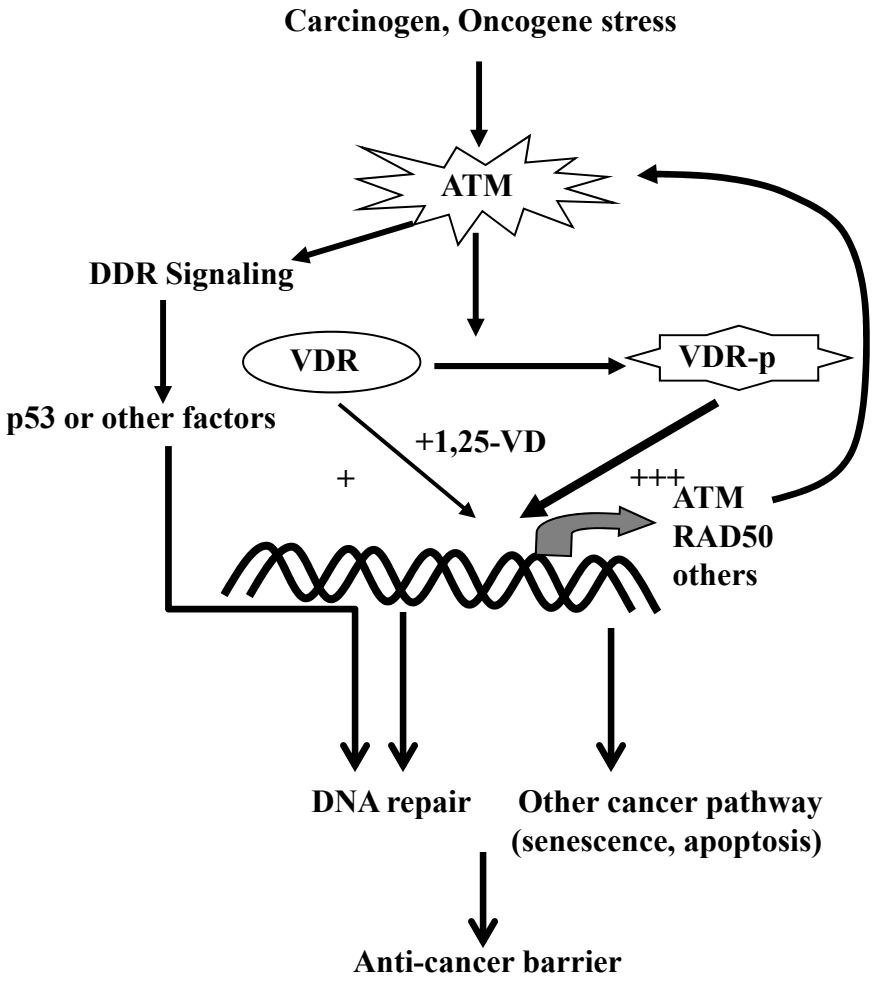
Carcinogen, Oncogene stress
ATM
DDR Signaling
VDR
VDR-p
p53 or other factors
+1,25-VD
+
+++
ATM
RAD50
others
DNA repair
Other cancer pathway
(senescence, apoptosis)
Anti-cancer barrier